



Repurposing Papaverine as an Antiviral Agent against Influenza Viruses and Paramyxoviruses

Megha Aggarwal,^{a,b} George P. Leser,^{a,b} Robert A. Lamb^{a,b}

^aDepartment of Molecular Biosciences, Northwestern University, Evanston, Illinois, USA

^bHoward Hughes Medical Institute, Northwestern University, Evanston, Illinois, USA

ABSTRACT Influenza viruses are highly infectious and are the leading cause of human respiratory diseases and may trigger severe epidemics and occasional pandemics. Although antiviral drugs against influenza viruses have been developed, there is an urgent need to design new strategies to develop influenza virus inhibitors due to the increasing resistance of viruses toward currently available drugs. In this study, we examined the antiviral activity of natural compounds against the following influenza virus strains: A/WSN/33 (H1N1), A/Udorn/72 (H3N2), and B/Lee/40. Papaverine (a nonnarcotic alkaloid that has been used for the treatment of heart disease, impotency, and psychosis) was found to be an effective inhibitor of multiple strains of influenza virus. Kinetic studies demonstrated that papaverine inhibited influenza virus infection at a late stage in the virus life cycle. An alteration in influenza virus morphology and viral ribonucleoprotein (vRNP) localization was observed as an effect of papaverine treatment. Papaverine is a well-known phosphodiesterase inhibitor and also modifies the mitogen-activated protein kinase (MAPK) pathway by downregulating the phosphorylation of MEK and extracellular signal-regulated kinase (ERK). Thus, the modulation of host cell signaling pathways by papaverine may be associated with the nuclear retention of vRNPs and the reduction of influenza virus titers. Interestingly, papaverine also inhibited paramyxoviruses parainfluenza virus 5 (PIV5), human parainfluenza virus 3 (HPIV3), and respiratory syncytial virus (RSV) infections. We propose that papaverine can be a potential candidate to be used as an antiviral agent against a broad range of influenza viruses and paramyxoviruses.

IMPORTANCE Influenza viruses are important human pathogens that are the causative agents of epidemics and pandemics. Despite the availability of an annual vaccine, a large number of cases occur every year globally. Here, we report that papaverine, a vasodilator, shows inhibitory action against various strains of influenza virus as well as the paramyxoviruses PIV5, HPIV3, and RSV. A significant effect of papaverine on the influenza virus morphology was observed. Papaverine treatment of influenza-virus-infected cells resulted in the inhibition of virus at a later time in the virus life cycle through the suppression of nuclear export of vRNP and also interfered with the host cellular cAMP and MEK/ERK cascade pathways. This study explores the use of papaverine as an effective inhibitor of both influenza viruses as well as paramyxoviruses.

KEYWORDS influenza virus, paramyxovirus, inhibitors, papaverine, phosphodiesterase, cAMP, MEK, ERK, MAPK, nuclear export, vRNP

Influenza viruses are responsible for highly contagious respiratory diseases leading to ~3 million deaths worldwide annually. The deadliest outbreak was in 1918; the so called Spanish flu (H1N1) led to 40 million to 50 million deaths (1). There was a record-breaking number of influenza-like diseases reported along with resulting hospitalizations in 2017 and 2018. Due to severe outbreaks and pandemics related to the

Citation Aggarwal M, Leser GP, Lamb RA. 2020. Repurposing papaverine as an antiviral agent against influenza viruses and paramyxoviruses. *J Virol* 94:e01888-19. <https://doi.org/10.1128/JVI.01888-19>.

Editor Rebecca Ellis Dutch, University of Kentucky College of Medicine

Copyright © 2020 American Society for Microbiology. All Rights Reserved.

Address correspondence to Robert A. Lamb, ralamb@northwestern.edu.

Received 5 November 2019
Accepted 20 December 2019

Accepted manuscript posted online 2 January 2020

Published 28 February 2020

influenza virus, it is necessary to identify means to limit or prevent the spread of the virus. An influenza vaccine is available annually. However, many individuals are not immunized, and even among the population receiving the vaccine, there are many cases per year worldwide due to the limitations of the seasonal influenza virus vaccines. At present, the available drugs effective for inhibiting influenza virus infection include neuraminidase inhibitors such as oseltamivir and zanamivir, agents such as amantadine and rimantadine that inhibit the M2 ion channel, and baloxavir that inhibits the polymerase acidic (PA) polymerase subunit of the virus by targeting its endonuclease activity (2). However, the seasonal influenza virus strains frequently exhibit resistance to these drugs (3–5). Hence, there is an urgent need to develop new antiviral drugs against influenza viruses.

Influenza virus replication and transcription occur in the nucleus of the host cell, and the ribonucleoprotein (RNP) complex consisting of nucleoprotein (NP) and viral genome assembles into virions in the cytoplasm (6). The virus infection cycle involves a bidirectional movement of RNP in and out of the nucleus; first, RNPs are imported into the nucleus for replication and transcription and, later, exported from the nucleus to the cytoplasm. After nuclear export, the genome is assembled and targeted toward the plasma membrane for virus budding. Therefore, the nuclear export of RNP is a crucial step in the virus propagation, and any delay in RNP export leads to a reduced viral titer (7–9). The process of nuclear export is mediated by various viral and host factors and signaling pathways (10–12).

Viruses are dependent on the host machinery for their infective life cycle, including virus attachment, entry, replication, and budding. Due to the increasing virus resistance against specific antiviral agents, drugs targeting host cell factors can be a very useful alternative for the inhibition of influenza virus. The extracellular signal-regulated kinase (ERK)/MEK and cAMP signaling pathways play an important role in the life cycle of various viruses (13–19). The mitogen-activated protein kinase (MAPK) cascade includes the Raf/MEK/ERK signaling pathway in which sequential phosphorylation/activation of these kinases takes place. Raf is a serine threonine kinase, and upon activation triggers the phosphorylation of MEK, which is a kinase with dual specificity (MAPK/ERK kinase). The activated MEK subsequently phosphorylates ERK, an extracellular signal-regulated kinase. This signaling pathway regulates the phosphorylation of various cellular transcription factors and, hence, gene expression, which further regulates cell differentiation, apoptosis, and inflammatory responses (20, 21). The role of the MAPK signaling pathway in the propagation of influenza virus infection has been described previously (17, 22).

Phosphodiesterases (PDEs) are a divergent superfamily of enzymes and are responsible for the hydrolysis of cyclic nucleotides cAMP and cyclic GMP (cGMP) and, thus, regulate their signaling pathways (23, 24). PDE4 is specific to the hydrolysis of cAMP. The inhibitors of PDE4 are effective in treating airway inflammatory diseases as well as influenza-induced lung inflammation (18, 25). PDE4 inhibitors rolipram and roflumilast have been described as effective antiviral agents against influenza virus and respiratory syncytial virus (RSV), respectively (18, 26). An increase in cAMP levels results in the reduction of RSV and measles virus growth (27, 28). In a recent study, a relationship between cAMP and MEK/ERK signaling pathways had been demonstrated, and a possible role of cAMP in the regulation of MEK/ERK activation was illustrated (29).

Papaverine is an alkaloid derived from isoquinoline found in the opium poppy plant (*Papaver somniferum*). Papaverine is a recognized inhibitor of phosphodiesterases (30, 31). It has been used for the treatment of heart diseases, as it acts as a vasodilator (32) and can be administered intraarterially for the treatment of cerebral vasospasm (33). Papaverine is utilized for the treatment of erectile dysfunction in males (34) and also acts as an antidepressant (35). Additionally, it exhibits an antitumor effect on human prostate cancer cells and glioblastoma cells (36, 37). Moreover, it has been reported to have an inhibitory effect on measles virus, cytomegalovirus (CMV), and human immunodeficiency virus (HIV) replication (38–40).

In this study, we investigated the anti-influenza activity of several natural com-

pounds and found that papaverine is a potent inhibitor of influenza virus infection. We have performed time kinetics studies to evaluate the stage of the virus life cycle at which inhibition occurs. The assays of hemagglutinin (HA) and neuraminidase (NA) activities were also performed in the presence and absence of papaverine. Also, to observe any possible effects of papaverine on virus morphology, purified virions were negatively stained and observed in an electron microscope. The effect of papaverine on the nuclear export of viral ribonucleoproteins (vRNPs) was examined. In addition, the intracellular levels of PDE4D/cAMP and MEK/ERK were demonstrated with and without papaverine. Furthermore, the antiviral action of papaverine was assessed upon cells infected with the following paramyxoviruses: parainfluenza virus 5 (PIV5), human parainfluenza virus 3 (HPIV3), RSV, or the rhabdovirus, vesicular stomatitis virus (VSV).

RESULTS

Identification of the compounds with anti-influenza activity. The primary goal of this work was to identify the potential of natural compounds as effective inhibitors of influenza or paramyxoviruses. Twelve natural compounds, apigenin, berberine, diosmetin, epicatechin, genistein, kaempferol, luteolin, myricetin, naringenin, oxybenzone, papaverine, and quercetin, were used in this study. These compounds were selected as they are naturally occurring plant derivatives and because of their known antiviral properties. The possible antiviral activities were evaluated at a concentration of 50 μ M against three strains of influenza virus, influenza A WSN/33 (H1N1) and Udorn/72 (H3N2) and influenza B Lee/40, by plaque reduction neutralization test (PRNT). We found that quercetin, papaverine, luteolin, and naringenin reduced the A/WSN/33 virus titer significantly. Quercetin, papaverine, and luteolin could also reduce the titer of the A/Udorn/72 strain (Fig. 1A). The compounds quercetin, papaverine, luteolin, kaempferol, diosmetin, and myricetin reduced the titer of the B/Lee/40 virus strain. However, epicatechin, oxybenzone, and genistein did not reduce the influenza virus titer. No compound resulted in observable cytotoxicity up to a 500 μ M concentration except apigenin and luteolin. Virus titer could not be measured for infected cultures treated with apigenin due to its high cytotoxicity (data not shown).

Papaverine exhibits strong anti-influenza activity. Papaverine was found to be an effective inhibitor of all three strains of influenza virus, so we focused on papaverine for further studies (Fig. 1B). MDCK or HEK293T cells were infected with influenza virus and grown in the presence of papaverine or dimethyl sulfoxide (DMSO). Virus was harvested, and virus titer was measured by plaque assays. Papaverine showed a dose-dependent inhibition of influenza virus strains used in this study (A/WSN/33, A/Udorn/72, A/Eq/2/Miami/1/63, B/Lee/40, and B/MD/59) (Fig. 1B and C and Table 1). The 50% inhibitory concentrations (IC_{50}) of papaverine for all of the virus strains are shown in Table 1. These results were also confirmed by the visualization of the virus-infected cells in the presence of papaverine by fluorescence microscopy. Cells infected with influenza virus strains were treated with various concentrations of papaverine and fixed at 24 hours postinfection (hpi). The cells were treated with anti-M2 and anti-hemagglutinin-neuraminidase (anti-HN) antibody for the influenza A and B virus, respectively. After the Alexa Fluor conjugated secondary antibody treatment, the coverslips were mounted with 4',6-diamidino-2-phenylindole (DAPI) and imaged by confocal microscope. The amount of viral proteins decreased in a dose-dependent manner relative to the papaverine concentration as shown by fluorescence staining (Fig. 1D), which is consistent with the results obtained from the plaque assays of harvested virus.

Papaverine acts at a late stage of influenza virus infection. The time of addition (TOA) and time of elimination (TOE) experiments were carried out to identify the step of inhibition in the virus life cycle. In TOA studies, papaverine was added at indicated time points following A/WSN/33 virus infection, and the titer of the harvested virus was analyzed using plaque assays (Fig. 2A). For TOE assays, papaverine was added at the start of virus infection and washed out at the indicated time points. For the pretreatment analysis, cells were incubated with papaverine 4 h prior to virus infection, and the

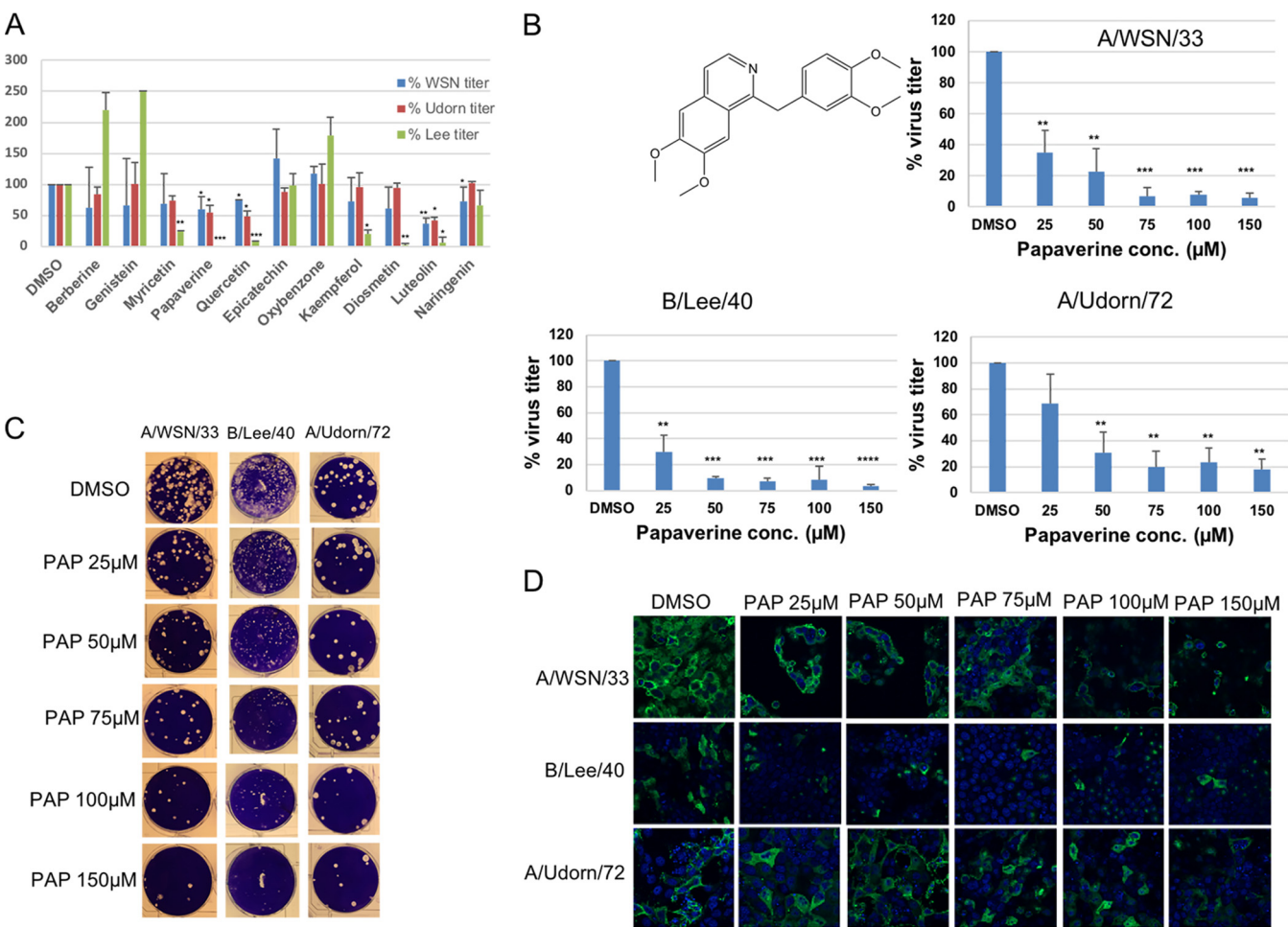


FIG 1 (A) Antiviral effect of compounds (50 μ M each) on influenza virus strains A/WSN/33 (H1N1) (blue), A/Udorn/72 (H3N2) (salmon), and B/Lee/40 (green). Data represent the average value of triplicate experiments with the standard deviation shown as error bars. (B) Molecular structure of papaverine (PAP) (drawn by ChemDraw [PerkinElmer Informatics]) and its effect on the growth of different influenza virus strains in a dose-dependent manner. (C) Virus growth in the presence of the indicated concentrations of papaverine was measured by plaque assay. The data represent one representative experiment of three replicates. The asterisk indicates statistical significance (*, $P < 0.05$; **, $P < 0.01$; ***, $P < 0.001$; ****, $P < 0.0001$). (D) Confocal microscopy analysis was performed with the cells infected with influenza virus and treated with various papaverine concentrations. The cells were fixed and stained with influenza A-specific M2 antibody or influenza B-specific HN antibody followed by Alexa Fluor 488 conjugated host-specific secondary antibody treatment. Virus is shown in green color, and DAPI staining is in blue.

compound was removed during infection by replacing the culture medium. The TOA experiment shows that papaverine causes a reduction in virus titer even if added 8 hpi (Fig. 2B). The TOE assay showed a decrease in the virus titer when papaverine was removed from the medium at a later time point of virus infection (Fig. 2C). It did not

TABLE 1 IC_{50} values of papaverine were calculated for various strains of influenza virus and paramyxoviruses

Influenza strain or virus	IC_{50} (μ M)
A/WSN/33 (H1N1)	16.77
B/Lee/40	14.34
A/Udorn/72 (H3N2)	36.41
A/Equine/2/MIAMI/1/63 (H3N8)	27.36
A/PR/8/34 (H1N1)	24.54
B/MD/59	2.63
RSV	2.02
PIV5	5.5
HPIV3	2.6
VSV	ND ^a

^aND, not determined.

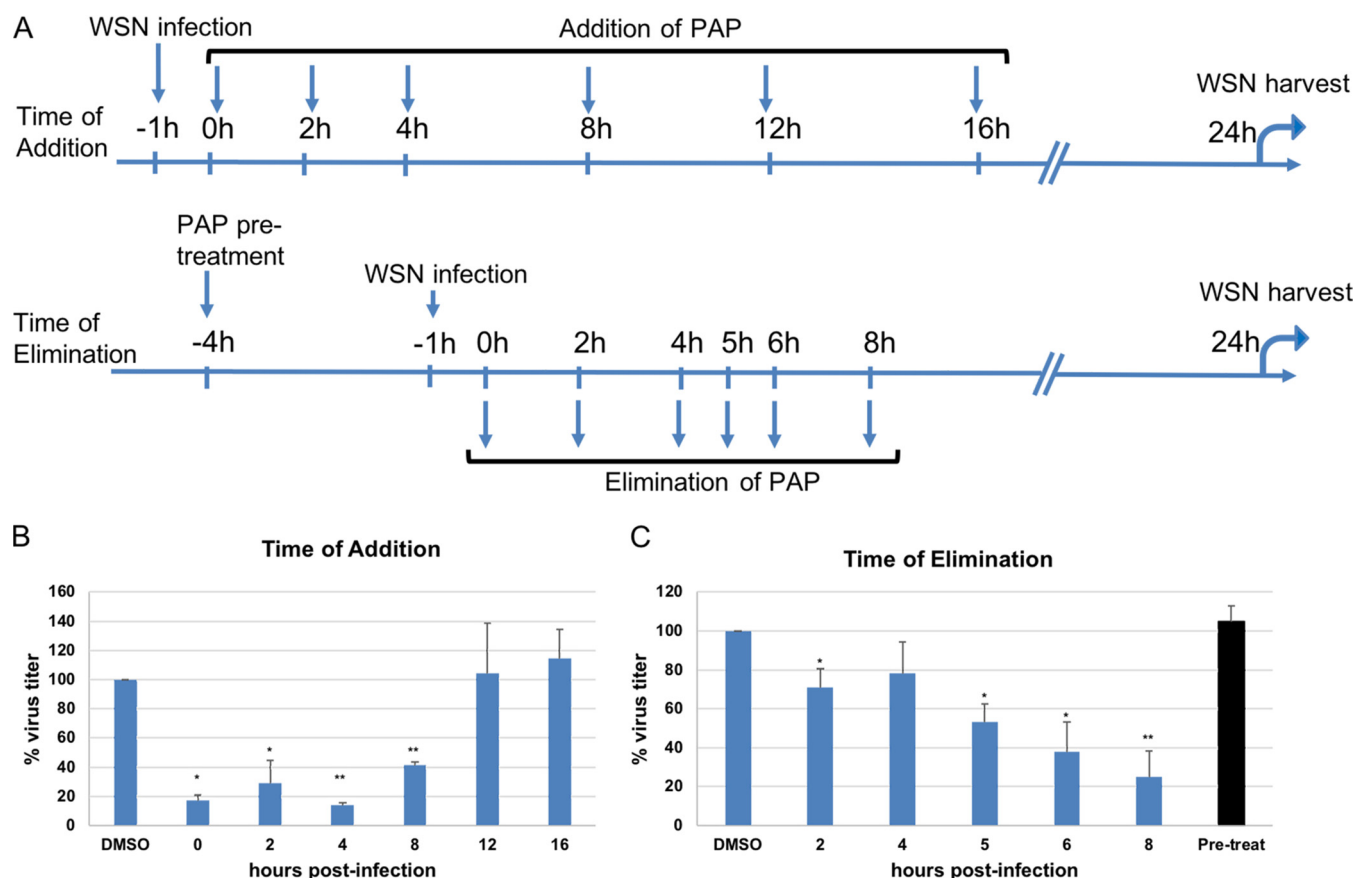


FIG 2 TOA and TOE assays were performed to identify the stage in the A/WSN/33 (H1N1) virus life cycle that is impacted by papaverine. (A) Schematic representation of the assays in which papaverine was added 0, 2, 4, 8, 12, or 16 hpi (top) or eliminated 0, 2, 4, 5, 6, or 8 hpi from the culture medium (bottom). For the pretreatment analysis, cells were treated with papaverine 4 h before virus infection, and culture medium was replaced with fresh medium without papaverine immediately after virus infection. Virus was harvested 24 hpi, and plaque assays were performed to calculate the virus titer. (B and C) The results of plaque assays are shown as the percentage of virus titer compared to that of the DMSO control. The pretreatment analysis bar is shown in black. The data denotes the mean \pm standard deviation from triplicate experiments. The asterisk indicates statistical significance (*, $P < 0.05$; **, $P < 0.01$).

show a significant reduction in virus titer when eliminated 4 hpi, although the reduction in virus titer was observed when papaverine was removed from infected cell cultures at ≥ 5 hpi. However, the addition of papaverine at 12 or 16 hpi did not cause a reduction in virus titer. The pretreatment of cells with papaverine did not inhibit virus infection. These results together imply that the inhibitory effect of papaverine occurs at a late stage of the influenza virus infection cycle.

The activity of HA/NA and viral RNA synthesis are not affected by papaverine treatment.

HA (hemagglutinin) and NA (neuraminidase) are essential proteins involved in the virus entry process through host receptor binding and the release of new virus particles via receptor-destroying activity, respectively (41). We evaluated the effect of papaverine on the activity of HA and NA proteins to examine if papaverine inhibited either entry or the release step of the virus life cycle. The A/WSN/33 virus strain was incubated in the presence of either papaverine or DMSO, and the activities of both HA and NA were measured. The NA activity was determined by measuring the intensity of the released fluorescent product 4-methylumbelliferone. The HA activity was assessed by observing its ability to cause the hemagglutination of chicken red blood cells (RBCs). Papaverine did not cause any difference in the activity of HA or NA surface glycoproteins of the virus (Fig. 3A and B). Further, viral RNA synthesis was analyzed by semiquantitative reverse transcriptase PCR (RT-PCR). Viral RNA was isolated from harvested virus grown in the presence of indicated concentrations of papaverine. The viral NP PCR gene segment reached a plateau at 38 cycles regardless of whether the virus

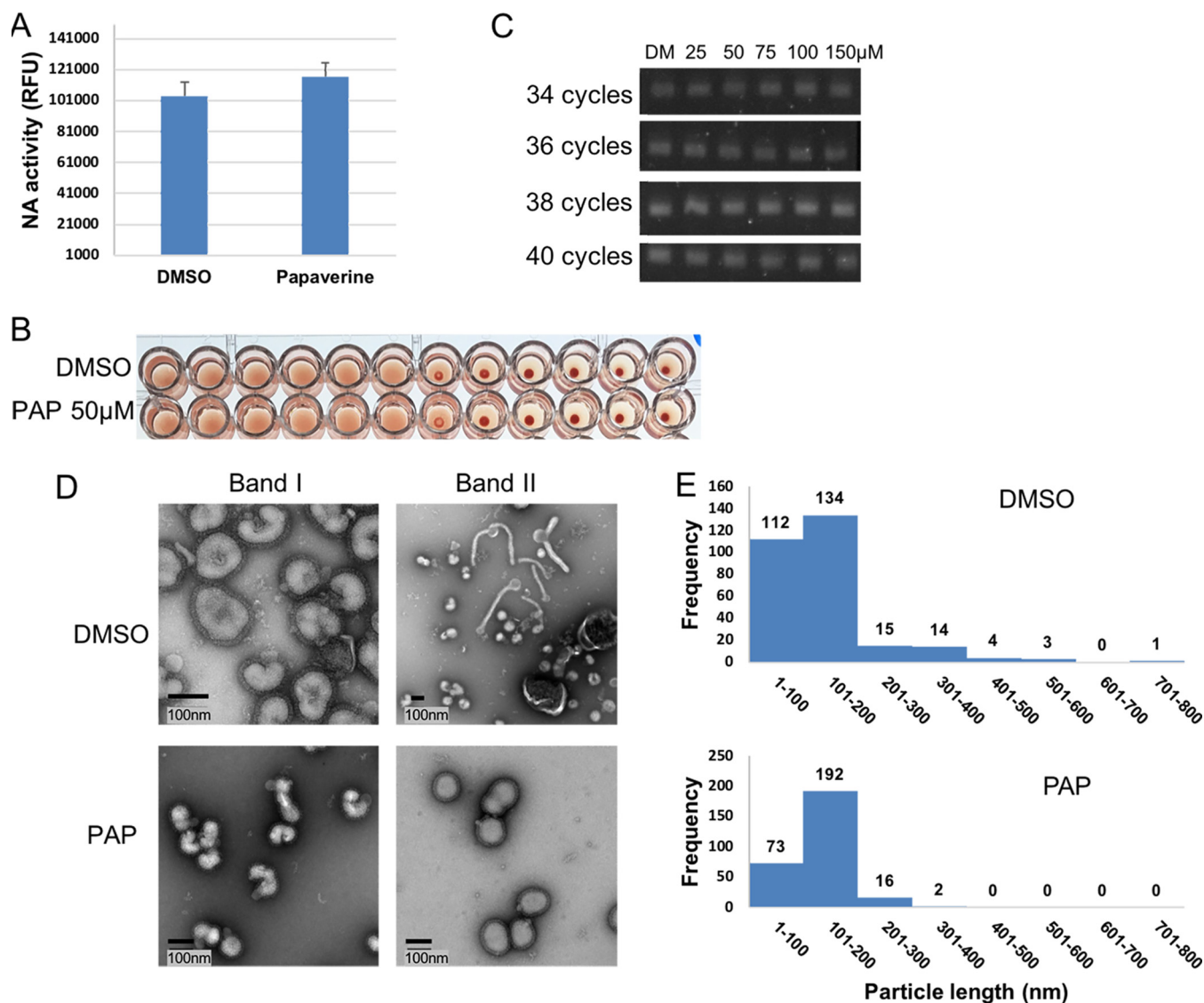


FIG 3 A/WSN/33 virus was incubated with either DMSO or papaverine for 1 h at 37°C. (A) The neuraminidase activity of the virus treated with DMSO or papaverine is displayed. The fluorescence intensity values were normalized with the control reaction. (B) The hemagglutination of RBCs by the virus with and without papaverine is shown. (C) Virus was grown with DMSO or papaverine at indicated concentrations, and semiquantitative RT-PCR was performed using the isolated RNA. The amplified products were collected at 34, 36, 38, and 40 cycles for each sample and analyzed by agarose gel electrophoresis. (D) Electron micrographs of negatively stained A/WSN/33 virus grown in the presence of DMSO (top) or papaverine (50 μ M) (bottom) are displayed. (E) The length of 280 particles was measured from each sample and the distribution of the length of the particles is shown.

was grown in the medium containing papaverine or DMSO. This suggests that papaverine does not affect influenza virus RNA synthesis (Fig. 3C).

Examination of influenza virus morphology in the presence or absence of papaverine. A/WSN/33 virus was grown in the presence of papaverine or DMSO and subsequently purified by centrifugation on sucrose gradients. The virions were collected and purified from each of the two major bands on the sucrose gradients, were absorbed onto the carbon-coated grids, and negatively stained. For virions grown in DMSO, band I contained virus particles exhibiting mostly a spherical morphology; however, predominantly filamentous virus particles were found in band II (Fig. 3D). Conversely, virions grown in medium containing papaverine were mostly spherical, and this was the case for virions purified from both gradient bands. The range of length observed for virus particles grown in the presence of papaverine was less than that for the virus grown with DMSO in the culture medium (Fig. 3E). For the virions grown in the presence of papaverine, most of the particles had a length that fell within the range of

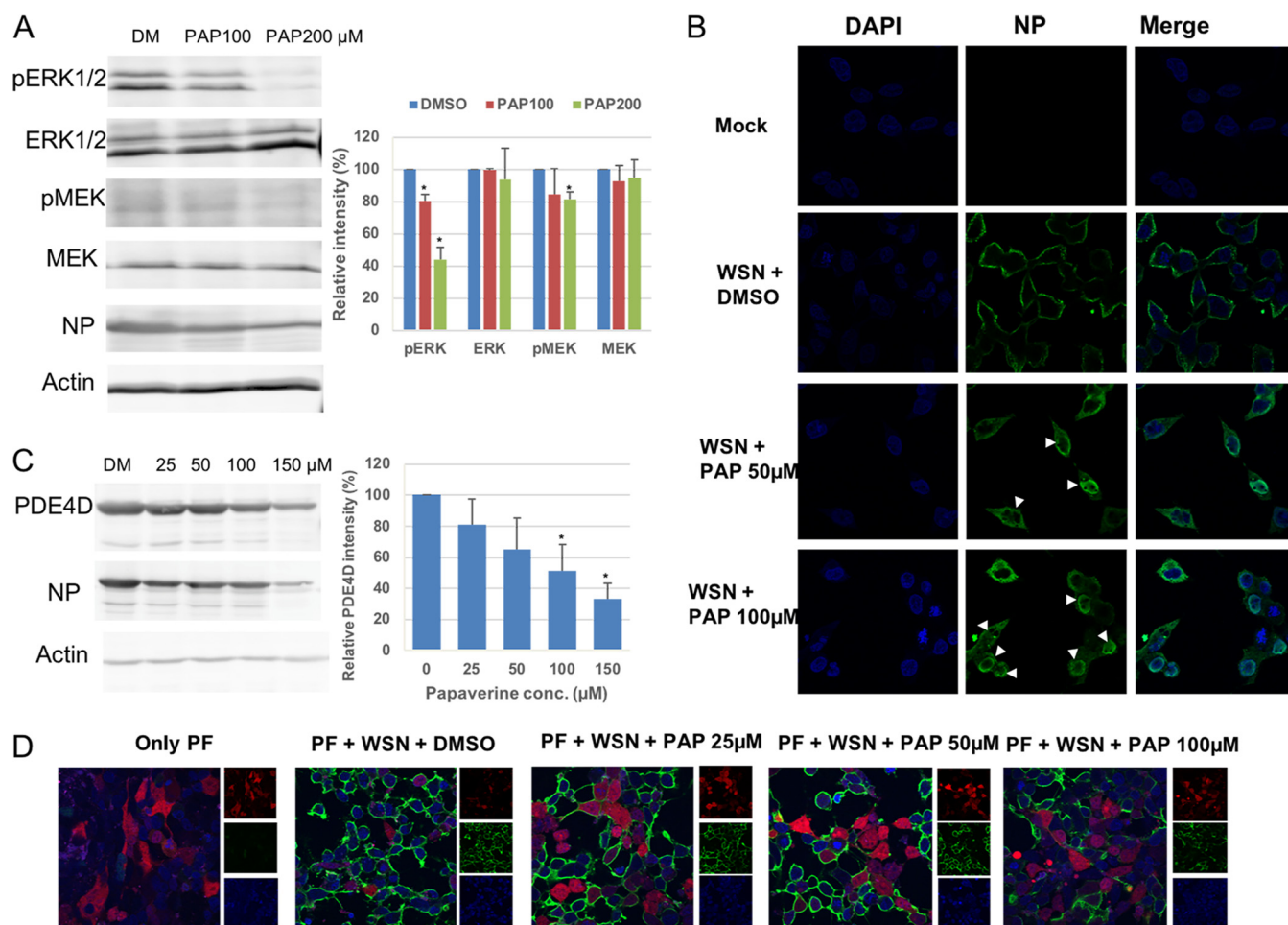


FIG 4 Papaverine interferes with the host cAMP and MEK/ERK signaling pathways and also inhibits viral nuclear export. (A) pERK, ERK, pMEK, MEK, NP, and actin levels are shown in HEK293T cells. The cells were infected with A/WSN/33 virus and treated with papaverine or DMSO. At 18 hpi, the cells were stimulated for an hour, lysed, and analyzed by Western blotting. The bands were quantified and the graph shows the mean protein levels calculated for triplicate experiments. The asterisk indicates statistical significance (*, $P < 0.05$). (B) Cells were infected with A/WSN/33 virus, papaverine treated, fixed at 8 hpi, and visualized with a confocal microscope. NP is rendered in green and the stained nuclei in blue. The nuclear accumulation of the vRNPs in papaverine-treated cells is shown by white arrows. (C) The level of PDE4D is shown in HEK293T cells infected with A/WSN/33 virus and treated with papaverine at the indicated concentrations. The blot shown here is the representative from the triplicate experiments, and the graph denotes the average of three independent experiments. (D) Confocal images of PF transfected HEK293T cells are displayed which were further infected with virus. The red color is the fluorescence signal from the PF reporter plasmid that proportionally corresponds to the cAMP level in the cells. The M2 protein of the A/WSN/33 virus is shown by green fluorescence, and the DAPI-stained nuclei is shown in blue. An increase in the fluorescent intensity of PF and a decrease in that of WSN M2 was observed with the increasing concentrations of papaverine.

101 to 200 nm. Whereas in the DMSO population, there was a broader range in length with an almost equal number of particles in the 1 to 100 and 101 to 200 ranges. Also, the virus population purified from the papaverine-treated cells had fewer filamentous particles than the DMSO samples.

Papaverine modulates MEK/ERK signaling pathway and also suppresses the nuclear export of vRNPs. To evaluate the effect of papaverine on the activation of MEK/ERK in infected cells, HEK293T cells were infected with A/WSN/33 virus and treated with either papaverine or DMSO. The cells were stimulated at 18 hpi, lysed after 1 h of stimulation, and analyzed by Western blotting. The phosphorylation of MEK and ERK was reduced in the presence of papaverine; however, the amount of MEK and ERK remains unchanged (Fig. 4A). Thus, our results suggest that papaverine alters the activation of the MEK/ERK pathway in 293T cells.

As the MEK/ERK signaling pathway has been proposed to play an important role in the nuclear export of vRNPs (15, 17), we postulated that papaverine may have an effect on the export of RNPs from the nucleus to the cytoplasm. The cellular localization of the

vRNPs was examined by the visualization of virus NP in the confocal microscope in HEK293T cells. The cells were infected with A/WSN/33 virus and treated with papaverine/DMSO. At 8 hpi, the cells were fixed and treated with anti-NP primary antibody followed by Alexa Fluor 488 conjugated secondary antibody. The coverslips were mounted with DAPI in the mounting medium and observed using a Zeiss LSM 800 confocal microscope. We found that NP was present in the cytoplasm in the DMSO-treated cells; however, most NP was localized in the nucleus after papaverine treatment, indicating its negative effect on the nuclear export of vRNPs (Fig. 4B). Thus, papaverine caused nuclear retention of the vRNPs at 8 hpi in influenza virus infection.

Papaverine interferes with the cAMP signaling pathway through inhibition of PDE4D. Intracellular levels of PDE4D were measured in HEK293T cells in the presence or absence of papaverine. Cells were infected with influenza virus, and papaverine (or DMSO) was added to the overlay medium. Cells were lysed 24 hpi, and the amount of PDE4D was determined by immunoblotting. The results showed a decrease in the PDE4D level upon treatment of cells with papaverine (Fig. 4C). This reduction is proportional to the papaverine concentration. Thus, a dose-dependent effect of papaverine on the PDE4D level was observed. There are several isoforms of PDE4D present in the cells; the band intensity for all observed isoforms of PDE4D decreased with an increase in papaverine concentration.

Since PDE4D is involved in the hydrolysis of cAMP, a reduction in the PDE4D activity by papaverine treatment would be anticipated corresponding to an increase in the amount of cellular cAMP (24). The levels of cAMP were evaluated using the plasmid Pink Flamindo (PF) (pink fluorescent cAMP indicator). PF consists of the red fluorescent protein mApple with an insertion of the cAMP binding domain of Epac1 (exchange protein activated by cAMP) (42). It has been reported to show an increase or decrease in fluorescence intensity in the presence of adenylyl cyclase activator or inhibitor, respectively. At 24 h posttransfection (hpt) with PF, cells were infected with influenza virus strain A/WSN/33 and overlaid with medium containing papaverine or DMSO. At 24 hpi, cells were fixed and stained with antibody (14C2) specific for the influenza virus protein M2. Cells were visualized by confocal microscopy for cAMP levels (red) and the presence of the M2 protein (green). The results showed that the amount of red fluorescence, indicative of cAMP levels, increases proportional to papaverine concentration (Fig. 4D).

Papaverine inhibits paramyxoviruses PIV5, HPIV3, and RSV but not VSV. The effect of papaverine treatment on cells infected with paramyxoviruses PIV5, RSV, and HPIV3 and rhabdovirus VSV was examined. The viruses were grown in the presence of various concentrations of papaverine or DMSO and then were harvested, 3 days postinfection (dpi) for PIV5, HPIV3, and RSV and 2 dpi for VSV. The harvested virus was titered by plaque assays, and IC_{50} values were calculated as shown in Table 1. PIV5, HPIV3, and RSV showed a reduced virus titer when grown in the presence of papaverine (Fig. 5A). However, VSV did not show an inhibition in virus titer after papaverine treatment, even at a concentration of 150 μ M. The results were confirmed by infecting CV-1 cells with either PIV5 or VSV that expressed green fluorescent protein (GFP). PIV5-GFP-infected cells treated with papaverine showed a proportional decrease in observed GFP fluorescence; however, the level of VSV-GFP fluorescence remains unchanged (Fig. 5B). Cell viability of CV-1 and HEp2 cells infected with HPIV3 and RSV, respectively, in the presence of papaverine was also observed using light microscopy. In both cases, a cytopathic effect was observed upon virus infection, which was significantly reduced when the viruses were grown with papaverine at the indicated concentrations (Fig. 5B).

DISCUSSION

Epidemics and pandemics resulting from influenza virus infection are a major threat to human health worldwide (1). The annual U.S. economic burden of influenza virus is significant. Although, a vaccine is available, influenza virus is still a major concern for public health globally. The increasing resistance of influenza viruses against currently

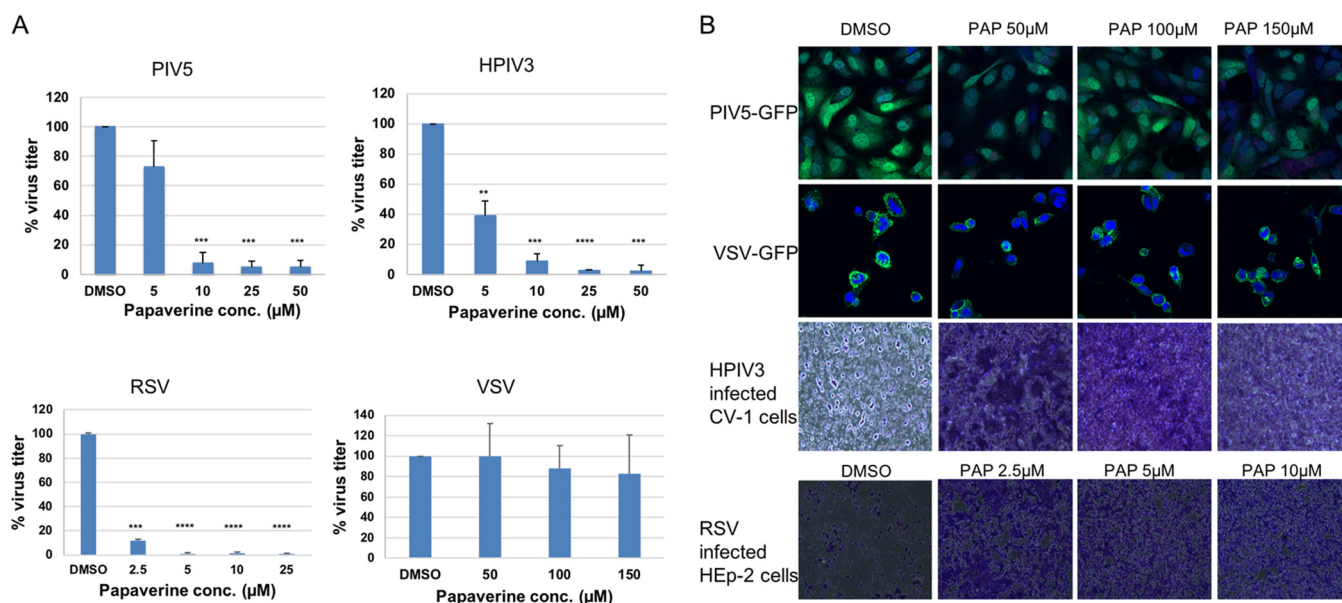


FIG 5 Antiviral effect of papaverine on paramyxoviruses PIV5, RSV, and HPIV3 and rhabdovirus VSV. (A) The percentage of virus titer with increasing concentration of papaverine. The graphs represent the mean values along with the standard deviation of triplicate experiments. The asterisk indicates statistical significance (*, $P < 0.05$; **, $P < 0.01$; ***, $P < 0.001$; ****, $P < 0.0001$). (B) Cells grown on coverslips were infected with PIV5-GFP or VSV-GFP and treated with papaverine or DMSO. The fluorescence signal was observed using a confocal microscope. The cells infected with viruses are rendered in green and DAPI in blue. CV-1 and HEP2 cells infected with HPIV3 and RSV, respectively, and treated with papaverine were stained with Hema-3 reagent, and the cytopathic effect was observed under a light microscope.

available antiviral drugs has brought about the urgent need of developing new strategies to counter influenza virus infection (4, 5). The focus of drug discovery has been directed mostly toward the inhibition of different viral proteins or the inhibition of virus entry (2, 43–46). However, there are also studies that provide insights into the development of antiviral agents targeting the host cellular signaling mechanism (18, 22, 28) or to enhance the antiviral response of host cells (47). Due to the fact that viruses are dependent on the host cell machinery for their life cycle and the comparatively low mutational rates of the host genes, targeting the host proteins can be a highly beneficial strategy for drug development against influenza virus. Inhibitors targeting the host cell signaling pathways could negatively affect cellular function and may lead to deleterious long-term and broad consequences. Hence, in our study, we used papaverine, which already has been in use for the treatment of various diseases in humans.

Our approach was to identify natural compounds that can be used as antiviral agents against a number of different strains of influenza virus. We found that at least seven of the selected compounds showed antiviral activity below cytotoxic concentrations (Fig. 1). Among those identified, papaverine was found to be a broadly effective inhibitor with very high efficacy and low cytotoxicity. The reduction in virus titer upon papaverine treatment was confirmed by fluorescence microscopy, HA assays, and plaque assays. Our results demonstrate that papaverine can be repurposed to be used as an antiviral agent against influenza virus infection. We have also investigated the inhibitory effect of papaverine against paramyxoviruses PIV5, RSV, and HPIV3 and rhabdovirus VSV. Human parainfluenza viruses and RSV are the major cause of lower respiratory tract infections in infants, young children, and immunocompromised adults (48). PIV5 has been used as a prototype to study paramyxoviruses (49). Papaverine dose dependently shows a significant inhibitory effect on the paramyxoviruses PIV5, RSV, and HPIV3. However, the growth of VSV was not reduced even at high concentrations of papaverine. Thus, papaverine causes a reduction in the titers of paramyxoviruses PIV5, RSV, and HPIV3 but not the rhabdovirus VSV.

Papaverine acts between 4 and 8 h post influenza virus infection and inhibits the

late stage of the virus life cycle as shown by time kinetics analysis. Thus, papaverine appears not to target either virus attachment or entry into host cells, consistent with the observations that neither HA nor NA activity of influenza virus A/WSN/33 was affected when the virus was incubated with papaverine outside the cells (Fig. 3). However, HA activity was reduced significantly when the virus was grown in cells treated with papaverine as a result of reduced virus titer (data not shown). Also, papaverine does not affect viral RNA synthesis as demonstrated by semiquantitative RT-PCR. We found that influenza virus morphology was affected by papaverine treatment. The presence of papaverine caused the particle length to be confined to a narrow range with mostly spherical or a few short filamentous virions, while particles with a greater range in length were found in the untreated population. However, the reason for this change in virus morphology by papaverine remains unknown.

Our results indicated that papaverine interferes with both cAMP and MEK/ERK signaling pathways in human cells in a dose-dependent manner. It has been shown previously that papaverine regulates the MEK/ERK pathway in retinal microglial cells through the cAMP signaling pathway (29). cAMP, a secondary messenger, has a key function in intracellular signaling, and its level inside the cells is regulated by PDEs. PDE4 inhibitors elevate cAMP level in the cells and have been used to treat respiratory diseases like asthma and chronic obstructive pulmonary diseases (23, 50). PDE4 is an important target for the treatment of central nervous system, inflammatory, and airway epithelial diseases (18, 23, 25, 50). Papaverine is a PDE4 inhibitor (30, 31) and also exhibits dose-dependent reduction of intracellular PDE4D levels in HEK293T cells (Fig. 4). Using a fluorescence-based approach, we demonstrated enhanced cAMP levels in the cells treated with papaverine compared to control. Furthermore, papaverine treatment reduces the phosphorylated MEK and ERK levels, while the concentrations of MEK and ERK are similar in treated and control cells. The activation of the MEK/ERK pathway is highly advantageous for virus replication, and the inhibitors of this pathway have been described as the inhibitors of influenza virus infection (14–17). In addition to influenza virus, other viruses including HIV, coronaviruses, RSV, CMV, and coxsackievirus B3 are also inhibited by MEK/ERK cascade inhibitors (51–55). Moreover, the inhibition of MEK pathway cascade by U0126 does not cause a negative effect on host cell viability, and similar results were observed with the use of papaverine (51). Thus, we suggest that the inhibition of the MAPK host cell signaling pathway may be responsible for the restriction of growth for a broad range of viruses. However, more detailed insight into the mechanism of the host signaling pathways and the interplay between host and viral factors is essential to better understand their function in viral infections.

The role of host factors in the viral life cycle remains elusive and is not completely understood. A relationship between MEK/ERK pathways and nuclear export of influenza virus RNPs has been established, as the inhibitors of this signaling pathway cause a delay/inhibition of nuclear export of viral RNA (14, 15, 17). The inhibition of ERK activation interferes with the nuclear export of vRNPs, which in turn restricts virus growth. Inhibitors of RNP nuclear export have been developed, which block influenza virus replication (7–9). Our results show nuclear accumulation of the vRNPs in papaverine-treated cells at 8 hpi compared to that of the DMSO control where almost all of the NPs are in the cytoplasm. Nuclear retention of the RNPs in the presence of papaverine suggests a possible mechanism of papaverine in virus inhibition. Also, the altered morphology of influenza virus particles when grown with papaverine might be the result of suppression of nuclear export of the viral genome; though there is still no direct evidence that links RNA nuclear export and viral morphology. There likely are other as yet unknown factors involved in the inhibition of virus infection by papaverine.

Thus, papaverine tends to influence the host signal transduction network through multiple factors linked to the MAPK pathway, which may be via cAMP signaling. Several other downstream and upstream factors might be involved in the mechanism of action.

Targeting the host cell pathways provides the additional benefit of preventing an increase in viral resistance to the antiviral agents. Further, the utilization of existing drugs makes the process of drug development safer and faster. In summary, our work

provides evidence for the effective inhibition of influenza virus by papaverine, likely through the suppression of nuclear export of vRNPs. The inhibition takes place via the host signaling pathways, including MEK/ERK and cAMP signaling cascades. The interplay among these two host cellular pathways and the transport of viral RNA have been demonstrated in previous studies. Taken together with prior findings, we propose that papaverine inhibits these cellular pathways in human cells, which likely impact the nuclear export of influenza virus RNA, an essential step in the virus life cycle.

MATERIALS AND METHODS

Cells and viruses. Human embryonic kidney cells (HEK293T), monkey kidney cells (CV-1), Madin-Darby bovine kidney (MDBK) cells, and Madin-Darby canine kidney (MDCK) cells were maintained in Dulbecco's modified Eagle's medium (DMEM) supplemented with 10% fetal bovine serum (FBS), penicillin, and streptomycin sulfate at 37°C. Human epithelial type 2 (HEp-2) cells were maintained in Eagle's minimum essential medium (EMEM) supplemented with FBS, penicillin, and streptomycin sulfate at 37°C. The influenza virus strains (A/WSN/33, A/Udorn/72, A/Eq/2/Miami/1/63, B/Lee/40, and B/MD/59) were propagated in MDCK or HEK293T cells. VSV and HPIV3 were grown in CV-1 cells. For the growth of RSV and PIV5 W3A, HEp2 and MDBK cells were used, respectively. All of the viruses were stored at -80°C and titered using plaque assays. Apigenin, berberine, diosmetin, epicatechin, genistein, kaempferol, luteolin, myricetin, naringenin, oxybenzone, papaverine, and quercetin were purchased from Sigma-Aldrich (St. Louis, MO).

Antiviral activity and plaque assay. Cells were plated in 12-well plates and infected with different viruses at a multiplicity of infection (MOI) of 0.1. Then, cells were incubated at 37°C for 1 h, virus was aspirated, and cells were overlaid with DMEM containing 2% FBS, antibiotics, and DMSO or the indicated compounds at specified concentrations. For influenza virus strains, the overlay medium also contained 1 µg/ml of *N*-acetylated trypsin to cleave hemagglutinin. After 2 dpi for influenza viruses and VSV and 3 dpi for other paramyxoviruses, the viruses were harvested, and plaque assays were performed to determine virus titers. After harvesting HPIV3 or RSV, cells were stained with Hema-3 reagent (Thermo Fisher Scientific, Inc.) and observed using an Evox XL inverted light microscope (Advanced Microscopy Group) to examine the cell cytopathic effect upon virus infection.

For plaque assays, harvested virus was serially diluted in DMEM and 1% bovine serum albumin (BSA). Cells were cultured in 6-well plates and upon confluence, infected with the appropriate dilution of virus. Incubations were done at 37°C for 1 h. Virus was removed, and cells were overlaid with DMEM containing antibiotics and 1.2% Avicel microcrystalline cellulose (FMC BioPolymer, Philadelphia, PA). Cells were incubated for several days (2 days for influenza viruses and VSV, 4 days for PIV5 and HPIV3, and 7 days for RSV). Overlaid medium was removed, and the cells were fixed with formaldehyde solution and stained with crystal violet. Plaques were counted to determine virus titer, and IC_{50} values were calculated using GraphPad Prism 7.00 for Mac (GraphPad Software, La Jolla, CA, USA).

PRNT and cytotoxicity assay. For PRNT, plaque assays were done as described above except the medium overlay contained either DMSO or papaverine, and the cells were incubated for 2 days. The overlay was removed, and the cells were stained with crystal violet for the visualization of plaques allowing the calculation of virus titer. For cytotoxicity assays, cells were cultured in 96-well plates and incubated with different concentrations of the compounds (up to 500 µM) for 3 days. alamarBlue cell viability reagent (Thermo Fisher Scientific, Inc.) was added, and the cells were further incubated at 37°C for 4 h. Absorbance was measured at 570 nm using a SpectraMax M5 plate reader (Molecular Devices, Sunnyvale, CA).

Semiquantitative RT-PCR. MDCK cells were infected with A/WSN/33 virus as described above and treated with DMSO or papaverine at specified concentrations (25 to 150 µM). At 24 hpi, virus was harvested, and RNA was isolated using Qiagen QIAamp viral RNA isolation minikit. PCR was performed with the isolated RNA using the SuperScript III one-step RT-PCR system with Platinum *Taq* high fidelity DNA polymerase (Invitrogen). Primers specific for WSN nucleoprotein were used, and PCR products were collected after 34, 36, 38, and 40 cycles. RT-PCR products were quantified after performing agarose gel electrophoresis.

Western blot assays. Cells were cultured in 6-well plates and infected with A/WSN/33 virus at an MOI of 5, and papaverine was added in the overlay medium at the indicated concentrations (25 to 200 µM). Cells were stimulated with cell stimulation cocktail containing phorbol myristate acetate (PMA) and ionomycin (Invitrogen) at 18 hpi for 1 h. Afterward, cells were lysed in SDS loading buffer and sonicated. Samples were boiled for 5 min and electrophoresed on 15% polyacrylamide SDS-PAGE. The gels were transferred to a polyvinylidene fluoride (PVDF) membrane, blocked with phosphate buffer saline (PBS) containing BSA, and incubated with primary antibodies (WSN rabbit polyclonal anti-NP, goat polyclonal anti-actin [Santa Cruz Biotechnology, Inc.], mouse monoclonal anti-PDE4D [ABclonal Technology], mouse monoclonal anti-pERK, anti-pMEK, anti-MEK [Santa Cruz Biotechnology, Inc.], or rabbit monoclonal anti-ERK [Cell Signaling Technology, Inc.]) followed by host-specific secondary immunoglobulins conjugated to Cy5 (Jackson ImmunoResearch, West Grove, PA). The reacted blots were visualized using a Typhoon FLA 9500 biomolecular imager (GE Healthcare Life Sciences), and the visible bands were quantified using ImageJ (56).

Virus purification and negative-stain electron microscopy. Cells were cultured in 10-cm dishes and infected with A/WSN/33 virus in the presence of 50 µM papaverine or DMSO. Viruses were harvested 2 days after infection and concentrated by centrifugation at $38,500 \times g$ for 45 min at 4°C using a

Beckman 70.1 Ti rotor (Beckman Coulter, Fullerton, CA). The pellet was resuspended in NTE (100 mM NaCl, 10 mM Tris pH 7.4, 1 mM EDTA), layered onto a 15% to 60% sucrose gradient, and centrifuged at $24,000 \times g$ for 1 h at 4°C using a Beckman SW 28 rotor. Purified virus was harvested, diluted in NTE, and pelleted again. The pelleted virus was resuspended in NTE and stored at -80°C until further use. Purified virus was diluted in NTE and applied to freshly glow-discharged carbon-coated grids. The grids were then stained with 2% uranyl formate and examined in a JEOL 1400 electron microscope operated at 120 kV. The images were collected with a Gatan ultrascan camera.

TOA and TOE assays. Cells were plated in 12-well plates and infected with A/WSN/33 virus as described above. TOA analysis was performed by the addition of papaverine (50 μ M) to the culture medium at 0, 2, 4, 6, 8, 12, and 16 hpi. For TOE assay, papaverine was added at the time of virus infection and the medium was aspirated and replaced with fresh medium lacking papaverine at 2, 4, 5, 6, and 8 hpi. For pretreatment analysis, cells were treated with papaverine 4 h before virus infection, and papaverine was removed during medium overlay after virus infection. At 24 hpi, virus was harvested, and the virus titers were determined using plaque assays.

Confocal microscopy. To perform the virus inhibition assay, cells were infected with influenza virus strains (A/WSN/33, A/Udorn/72, or B/Lee) or viruses engineered to express green fluorescent protein (GFP) (PIV5-GFP or VSV-GFP) as indicated. For the determination of cAMP levels, HEK293T cells were cultured on glass coverslips in 6-well plates and transfected with the plasmid Pink Flamindo (PF) (gifted from Tetsuya Kitaguchi [Addgene plasmid no. 102356]) (42) using lipofectamine and Plus reagent (Invitrogen) according to the manufacturer's protocol. At 24 hpi, the PF transfected cells were infected with A/WSN/33 virus and overlaid with medium containing papaverine or DMSO. After the indicated time point, virus was aspirated off and cells were fixed with 4% formaldehyde solution in phosphate buffer for 15 min. Cells were blocked with 3% BSA and permeabilized with 0.05% saponin and then reacted with primary antibodies as indicated (influenza A-specific mouse monoclonal 14C2 anti-M2, rabbit polyclonal anti-NP, or goat polyclonal B/Lee/40 anti-HA) followed by host-specific Alexa Fluor conjugated secondary antibodies. Then the coverslips were mounted on the slides using Prolong gold antifade reagent with DAPI (Thermo Fisher Scientific, Inc.). Cells were visualized using a Zeiss LSM 800 confocal microscope (Carl Zeiss Microscopy).

Hemagglutination and Neuraminidase activity inhibition assays. The HA inhibition assay was performed by incubating the virus with either 50 μ M papaverine or DMSO for 1 h at 37°C. Virus was serially diluted in PBS in a 96-well plate and an equal amount of 0.7% chicken RBCs (stored in Alsever's solution) was added. The plate was incubated for an hour at 4°C and analyzed visually for RBC agglutination.

To measure NA inhibition activity, virus was incubated with papaverine or DMSO at 37°C for 1 h in a black-walled 96-well plate. A total of 100 μ M of the fluorogenic neuraminidase substrate MUNANA (4-methylumbelliferyl-*N*-acetyl- α -D-neuraminic acid) (Sigma-Aldrich, St. Louis, MO) was added, and the reaction was allowed to proceed at 37°C for 2 h. The reaction was stopped by the addition of 0.014 N NaOH in 83% ethanol. The fluorescence generated by the cleaved substrate was measured at the excitation and emission wavelengths of 365 and 460 nm, respectively, using a SpectraMax M5 plate reader (Molecular Devices, Sunnyvale, CA). The fluorescence intensity values were normalized using a control reaction without virus.

ACKNOWLEDGMENT

M.A. is an Associate, G.P.L. is a specialist, and R.A.L. is an investigator of Howard Hughes Medical Institute.

We thank the cryo-electron microscopy facility at Northwestern University, Evanston, IL.

REFERENCES

1. Taubenberger JK, Morens DM. 2006. 1918 influenza: the mother of all pandemics. *Emerg Infect Dis* 12:15–22. <https://doi.org/10.3201/eid1201.050979>.
2. O'Hanlon R, Shaw ML. 2019. Baloxavir marboxil: the new influenza drug on the market. *Curr Opin Virol* 35:14–18. <https://doi.org/10.1016/j.coviro.2019.01.006>.
3. de Jong MD, Tran TT, Truong HK, Vo MH, Smith GJ, Nguyen VC, Bach VC, Phan TQ, Do QH, Guan Y, Peiris JS, Tran TH, Farrar J. 2005. Oseltamivir resistance during treatment of influenza A (H5N1) infection. *N Engl J Med* 353:2667–2672. <https://doi.org/10.1056/NEJMoa054512>.
4. Leonov H, Astrahan P, Krugliak M, Arkin IT. 2011. How do aminoadamantanes block the influenza M2 channel, and how does resistance develop? *J Am Chem Soc* 133:9903–9911. <https://doi.org/10.1021/ja202288m>.
5. McKimm-Breschkin JL. 2000. Resistance of influenza viruses to neuraminidase inhibitors—a review. *Antiviral Res* 47:1–17. [https://doi.org/10.1016/S0166-3542\(00\)00103-0](https://doi.org/10.1016/S0166-3542(00)00103-0).
6. Boulo S, Akarsu H, Ruigrok RWH, Baudin F. 2007. Nuclear traffic of influenza virus proteins and ribonucleoprotein complexes. *Virus Res* 124:12–21. <https://doi.org/10.1016/j.virusres.2006.09.013>.
7. He J, Qi W, Wang L, Tian J, Jiao P, Liu G, Ye W, Liao M. 2013. Amaryllidaceae alkaloids inhibit nuclear-to-cytoplasmic export of ribonucleoprotein (RNP) complex of highly pathogenic avian influenza virus H5N1. *Influenza Other Respir Viruses* 7:922–931. <https://doi.org/10.1111/irv.12035>.
8. Perwitasari O, Johnson S, Yan X, Howerth E, Shacham S, Landesman Y, Baloglu E, McCauley D, Tamir S, Tompkins SM, Tripp RA. 2014. Verdinexor, a novel selective inhibitor of nuclear export, reduces influenza A virus replication in vitro and in vivo. *J Virol* 88:10228–10243. <https://doi.org/10.1128/JVI.01774-14>.
9. Zheng W, Fan W, Zhang S, Jiao P, Shang Y, Cui L, Mahesutihan M, Li J, Wang D, Gao GF, Sun L, Liu W. 2019. Naproxen exhibits broad anti-influenza virus activity in mice by impeding viral nucleoprotein nuclear export. *Cell Rep* 27:1875–1885. <https://doi.org/10.1016/j.celrep.2019.04.053>.
10. Furusawa Y, Yamada S, Kawaoka Y. 2018. Host factor nucleoporin 93 is

- involved in the nuclear export of influenza virus RNA. *Front Microbiol* 9:1675. <https://doi.org/10.3389/fmicb.2018.01675>.
11. Qiao Y, Yan Y, Tan KS, Seet JE, Arumugam TV, Chow VTK, Wang DY, Tran T. 2018. CD151, a novel host factor of nuclear export signaling in influenza virus infection. *J Allergy Clin Immunol* 141:1799–1817. <https://doi.org/10.1016/j.jaci.2017.11.032>.
 12. Satterly N, Tsai P-L, Van Deursen J, Nussenzveig DR, Wang Y, Faria PA, Levay A, Levy DE, Fontoura B. 2007. Influenza virus targets the mRNA export machinery and the nuclear pore complex. *Proc Natl Acad Sci U S A* 104:1853–1858. <https://doi.org/10.1073/pnas.0610977104>.
 13. Coon TA, McKelvey AC, Weatherington NM, Birru RL, Lear T, Leikauf GD, Chen BB. 2014. Novel PDE4 inhibitors derived from Chinese medicine forsythia. *PLoS One* 9:e115937. <https://doi.org/10.1371/journal.pone.0115937>.
 14. Droebe K, Pleschka S, Ludwig S, Planz O. 2011. Antiviral activity of the MEK-inhibitor U0126 against pandemic H1N1v and highly pathogenic avian influenza virus in vitro and in vivo. *Antiviral Res* 92:195–203. <https://doi.org/10.1016/j.antiviral.2011.08.002>.
 15. Ludwig S, Wolff T, Ehrhardt C, Wurzer WJ, Reinhardt J, Planz O, Pleschka S. 2004. MEK inhibition impairs influenza B virus propagation without emergence of resistant variants. *FEBS Lett* 561:37–43. [https://doi.org/10.1016/S0014-5793\(04\)00108-5](https://doi.org/10.1016/S0014-5793(04)00108-5).
 16. Pinto R, Herold S, Cakarova L, Hoegner K, Lohmeyer J, Planz O, Pleschka S. 2011. Inhibition of influenza virus-induced NF- κ B and Raf/MEK/ERK activation can reduce both virus titers and cytokine expression simultaneously in vitro and in vivo. *Antiviral Res* 92:45–56. <https://doi.org/10.1016/j.antiviral.2011.05.009>.
 17. Pleschka S, Wolff T, Ehrhardt C, Hobom G, Planz O, Rapp UR, Ludwig S. 2001. Influenza virus propagation is impaired by inhibition of the Raf/MEK/ERK signalling cascade. *Nat Cell Biol* 3:301–305. <https://doi.org/10.1038/35060098>.
 18. Sharma G, Sharma DC, Fen LH, Pathak M, Bethur N, Pendharkar V, Peiris M, Altmeyer R. 2013. Reduction of influenza virus-induced lung inflammation and mortality in animals treated with a phosphodiesterase-4 inhibitor and a selective serotonin reuptake inhibitor. *Emerg Microbes Infect* 2:e54. <https://doi.org/10.1038/emi.2013.52>.
 19. Xing Z, Cardona CJ, Anunciacion J, Adams S, Dao N. 2010. Roles of the ERK MAPK in the regulation of proinflammatory and apoptotic responses in chicken macrophages infected with H9N2 avian influenza virus. *J Gen Virol* 91:343–351. <https://doi.org/10.1099/vir.0.015578-0>.
 20. Pearson G, Robinson F, Beers Gibson T, Xu B, Karandikar M, Berman K, Cobb MH. 2001. Mitogen-activated protein (MAP) kinase pathways: regulation and physiological functions. *Endocr Rev* 22:153–183. <https://doi.org/10.1210/edrv.22.2.0428>.
 21. Su B, Karin M. 1996. Mitogen-activated protein kinase cascades and regulation of gene expression. *Curr Opin Immunol* 8:402–411. [https://doi.org/10.1016/S0952-7915\(96\)80131-2](https://doi.org/10.1016/S0952-7915(96)80131-2).
 22. Dong W, Wei X, Zhang F, Hao J, Huang F, Zhang C, Liang W. 2014. A dual character of flavonoids in influenza A virus replication and spread through modulating cell-autonomous immunity by MAPK signaling pathways. *Sci Rep* 4:7237. <https://doi.org/10.1038/srep07237>.
 23. Houslay MD, Schafer P, Zhang K. 2005. Keynote review: phosphodiesterase-4 as a therapeutic target. *Drug Discov Today* 10:1503–1519. [https://doi.org/10.1016/S1359-6446\(05\)03622-6](https://doi.org/10.1016/S1359-6446(05)03622-6).
 24. Houslay MD, Adams DR. 2003. PDE4 cAMP phosphodiesterases: modular enzymes that orchestrate signalling cross-talk, desensitization and compartmentalization. *Biochem J* 370:1–18. <https://doi.org/10.1042/BJ20021698>.
 25. Lagente V, Martin-Chouly C, Boichot E, Martins MA, Silva P. 2005. Selective PDE4 inhibitors as potent anti-inflammatory drugs for the treatment of airway diseases. *Mem Inst Oswaldo Cruz* 100:131–136. <https://doi.org/10.1590/S0074-0276200500900023>.
 26. Mata M, Martinez I, Melero JA, Tenor H, Cortijo J. 2013. Roflumilast inhibits respiratory syncytial virus infection in human differentiated bronchial epithelial cells. *PLoS One* 8:e69670. <https://doi.org/10.1371/journal.pone.0069670>.
 27. Rezaee F, Harford TJ, Linfield DT, Altawallbeh G, Midura RJ, Ivanov AI, Piedimonte G. 2017. cAMP-dependent activation of protein kinase A attenuates respiratory syncytial virus-induced human airway epithelial barrier disruption. *PLoS One* 12:e0181876. <https://doi.org/10.1371/journal.pone.0181876>.
 28. Robbins SJ, Rapp F. 1980. Inhibition of measles virus replication by cyclic AMP. *Virology* 106:317–326. [https://doi.org/10.1016/0042-6822\(80\)90255-x](https://doi.org/10.1016/0042-6822(80)90255-x).
 29. Zhou T, Zhu Y. 2019. Cascade signals of papaverine inhibiting LPS-induced retinal microglial activation. *J Mol Neurosci* 68:111–119. <https://doi.org/10.1007/s12031-019-01289-w>.
 30. Pösch G, Kukovetz WR. 1971. Papaverine-induced inhibition of phosphodiesterase activity in various mammalian tissues. *Life Sci* 10:133–144. [https://doi.org/10.1016/0024-3205\(71\)90086-5](https://doi.org/10.1016/0024-3205(71)90086-5).
 31. Triner L, Vulliamoz Y, Schwartz I, Nahas GG. 1970. Cyclic phosphodiesterase activity and the action of papaverine. *Biochem Biophys Res Commun* 40:64–69. [https://doi.org/10.1016/0006-291x\(70\)91046-6](https://doi.org/10.1016/0006-291x(70)91046-6).
 32. Wilson RF, White CW. 1986. Intracoronary papaverine: an ideal coronary vasodilator for studies of the coronary circulation in conscious humans. *Circulation* 73:444–451. <https://doi.org/10.1161/01.cir.73.3.444>.
 33. Marks MP, Steinberg GK, Lane B. 1993. Intraarterial papaverine for the treatment of vasospasm. *AJNR Am J Neuroradiol* 14:822–826.
 34. Virag R. 1982. Intracavernous injection of papaverine for erectile failure. *Lancet* 2:938. [https://doi.org/10.1016/S0140-6736\(82\)90910-2](https://doi.org/10.1016/S0140-6736(82)90910-2).
 35. Malison RT, Price LH, Nestler EJ, Heninger GR, Duman RS. 1997. Efficacy of papaverine addition for treatment-refractory major depression. *Am J Psychiatry* 154:579–580. <https://doi.org/10.1176/ajp.154.4.579>.
 36. Huang H, Li L-J, Zhang H-B, Wei A-Y. 2017. Papaverine selectively inhibits human prostate cancer cell (PC-3) growth by inducing mitochondrial mediated apoptosis, cell cycle arrest and downregulation of NF- κ B/PI3K/Akt signalling pathway. *J BUON* 22:112–118.
 37. Inada M, Shindo M, Kobayashi K, Sato A, Yamamoto Y, Akasaki Y, Ichimura K, Tanuma S. 2019. Anticancer effects of a non-narcotic opium alkaloid medicine, papaverine, in human glioblastoma cells. *PLoS One* 14:e0216358. <https://doi.org/10.1371/journal.pone.0216358>.
 38. Albrecht T, Lee C-H, Speelman DJ, Steinsland OS. 1987. Inhibition of cytomegalovirus replication by smooth-muscle relaxing agents. *Proc Soc Exp Biol Med* 186:41–46. <https://doi.org/10.3181/00379727-186-42581>.
 39. Nokta M, Albrecht T, Pollard R. 1993. Papaverine hydrochloride: effects on HIV replication and T-lymphocyte cell function. *Immunopharmacology* 26:181–185. [https://doi.org/10.1016/0162-3109\(93\)90010-n](https://doi.org/10.1016/0162-3109(93)90010-n).
 40. Yoshikawa Y, Yamanouchi K. 1984. Effect of papaverine treatment on replication of measles virus in human neural and nonneural cells. *J Virol* 50:489–496.
 41. Gamblin SJ, Skehel JJ. 2010. Influenza hemagglutinin and neuraminidase membrane glycoproteins. *J Biol Chem* 285:28403–28409. <https://doi.org/10.1074/jbc.R110.129809>.
 42. Harada K, Ito M, Wang X, Tanaka M, Wongso D, Konno A, Hirai H, Hirase H, Tsuboi T, Kitaguchi T. 2017. Red fluorescent protein-based cAMP indicator applicable to optogenetics and in vivo imaging. *Sci Rep* 7:7351. <https://doi.org/10.1038/s41598-017-07820-6>.
 43. Aggarwal M, Tapas S, Siwach A, Kumar P, Kuhn RJ, Tomar S. 2012. Crystal structure of influenza A virus capsid protease and its complex with dioxane: new insights into capsid-glycoprotein molecular contacts. *PLoS One* 7:e51288. <https://doi.org/10.1371/journal.pone.0051288>.
 44. Aggarwal M, Sharma R, Kumar P, Parida M, Tomar S. 2015. Kinetic characterization of trans-proteolytic activity of Chikungunya virus capsid protease and development of a FRET-based HTS assay. *Sci Rep* 5:14753. <https://doi.org/10.1038/srep14753>.
 45. Chen X, Si L, Liu D, Proksch P, Zhang L, Zhou D, Lin W. 2015. Neoechinulin B and its analogues as potential entry inhibitors of influenza viruses, targeting viral hemagglutinin. *Eur J Med Chem* 93:182–195. <https://doi.org/10.1016/j.ejmech.2015.02.006>.
 46. Wu W, Li R, Li X, He J, Jiang S, Liu S, Yang J. 2015. Quercetin as an antiviral agent inhibits influenza A virus (IAV) entry. *Viruses* 8:6. <https://doi.org/10.3390/v8010006>.
 47. Li Z, Zhao J, Zhou H, Li L, Ding Y, Li J, Zhou B, Jiang H, Zhong N, Hu W, Yang Z. 2018. Capparilioside A shows antiviral and better anti-inflammatory effects against influenza virus via regulating host IFN signaling, in vitro and in vivo. *Life Sci* 200:115–125. <https://doi.org/10.1016/j.lfs.2018.03.033>.
 48. Wendt CH, Hertz MI. 1995. Respiratory syncytial virus and parainfluenza virus infections in the immunocompromised host. *Semin Respir Infect* 10:224–231.
 49. Aggarwal M, Leser GP, Kors CA, Lamb RA. 2018. Structure of the paramyxovirus parainfluenza virus 5 nucleoprotein in complex with an amino-terminal peptide of the phosphoprotein. *J Virol* 92:e01304-17. <https://doi.org/10.1128/JVI.01304-17>.
 50. Kodimuthali A, Jabari SSL, Pal M. 2008. Recent advances on phosphodiesterase 4 inhibitors for the treatment of asthma and chronic obstructive

- pulmonary disease. *J Med Chem* 51:5471–5489. <https://doi.org/10.1021/jm800582j>.
51. Cai Y, Liu Y, Zhang X. 2007. Suppression of coronavirus replication by inhibition of the MEK signaling pathway. *J Virol* 81:446–456. <https://doi.org/10.1128/JVI.01705-06>.
 52. Gong J, Shen X, Chen C, Qiu H, Yang R. 2011. Down-regulation of HIV-1 infection by inhibition of the MAPK signaling pathway. *Virol Sin* 26: 114–122. <https://doi.org/10.1007/s12250-011-3184-y>.
 53. Johnson RA, Ma X-L, Yurochko AD, Huang E-S. 2001. The role of MKK1/2 kinase activity in human cytomegalovirus infection. *J Gen Virol* 82: 493–497. <https://doi.org/10.1099/0022-1317-82-3-493>.
 54. Kong X, San Juan H, Behera A, Peebles ME, Wu J, Lockey RF, Mohapatra SS. 2004. ERK-1/2 activity is required for efficient RSV infection. *FEBS Lett* 559:33–38. [https://doi.org/10.1016/S0014-5793\(04\)00002-X](https://doi.org/10.1016/S0014-5793(04)00002-X).
 55. Luo H, Yanagawa B, Zhang J, Luo Z, Zhang M, Esfandiarei M, Carthy C, Wilson JE, Yang D, McManus BM. 2002. Coxsackievirus B3 replication is reduced by inhibition of the extracellular signal-regulated kinase (ERK) signaling pathway. *J Virol* 76:3365–3373. <https://doi.org/10.1128/jvi.76.7.3365-3373.2002>.
 56. Schindelin J, Arganda-Carreras I, Frise E, Kaynig V, Longair M, Pietzsch T, Preibisch S, Rueden C, Saalfeld S, Schmid B, Tinevez J-Y, White DJ, Hartenstein V, Eliceiri K, Tomancak P, Cardona A. 2012. Fiji: an open-source platform for biological-image analysis. *Nat Methods* 9:676–682. <https://doi.org/10.1038/nmeth.2019>.